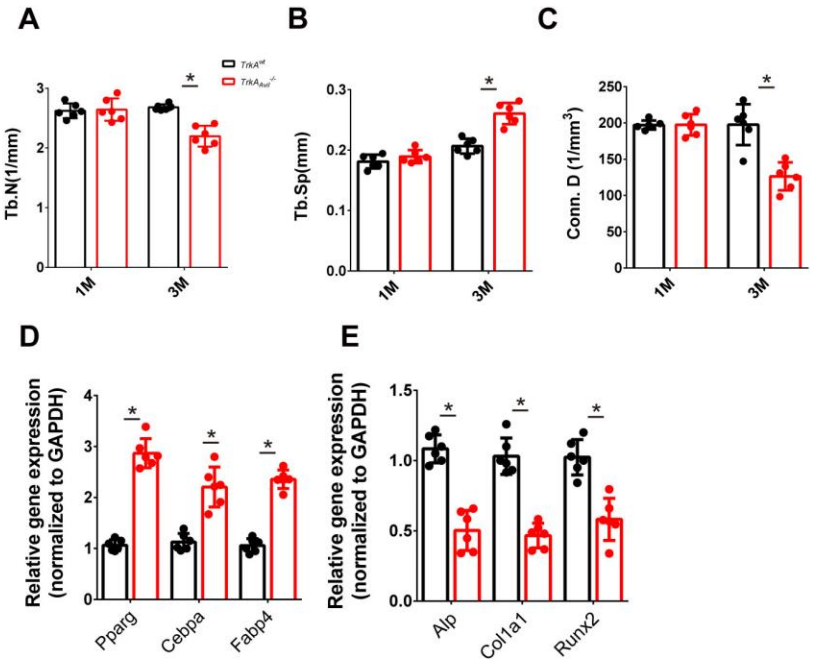

Supplemental Figure 1:

(A–C) Quantitative analysis of trabecular number (Tb. N), trabecular separation (Tb.Sp) and connectivity density (Conn. D) from 1-month-old and 3-month-old male *TrkA*^{wt} and *TrkA*$_{Avil}^{-/-}$ mice. (D-E) qPCR analysis of adipogenesis- and osteogenesis-related gene expression expression in MSCs isolated from 3-month-old male *TrkA*^{wt} and *TrkA*$_{Avil}^{-/-}$ mice. N≥6 per group, **P*<0.05 (Student t-test).

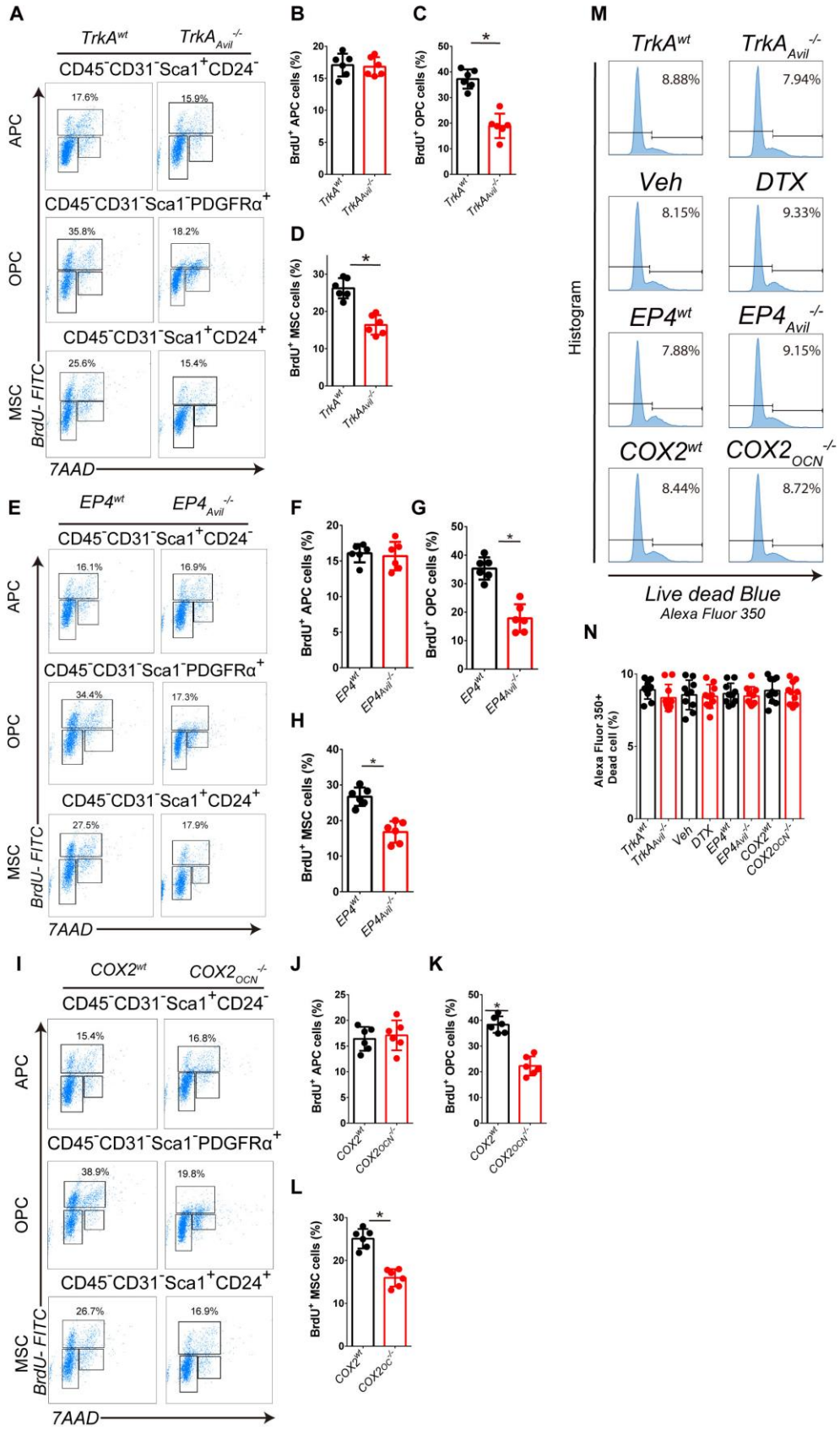
A
TrkA^wt
TrkA_Avil^-/-
CD45-CD31-Sca1+CD24-
17.6%
15.9%
APC
CD45-CD31-Sca1-PDGFRα+
35.8%
18.2%
OPC
CD45-CD31-Sca1+CD24+
25.6%
15.4%
MSC
BrdU- FITC
7AAD
B
BrdU+ APC cells (%)
C
BrdU+ OPC cells (%)
D
BrdU+ MSC cells (%)
E
EP4^wt
EP4_Avil^-/-
16.1%
16.9%
34.4%
17.3%
27.5%
17.9%
F
G
H
I
COX2^wt
COX2_OCN^-/-
15.4%
16.8%
38.9%
19.8%
26.7%
16.9%
J
K
L
M
Histogram
8.88%
7.94%
Veh
DTX
8.15%
9.33%
7.88%
9.15%
8.44%
8.72%
Live dead Blue
Alexa Fluor 350
N
Alexa Fluor 350+ Dead cell (%)

Supplemental Figure 2:

(A) Representative dot plot images of flow cytometry for $BrdU^+$ incorporation, top box gate of the plot image represents FITC labeled $BrdU^+$ cells. (B-D) quantitative analysis of $BrdU^+$ incorporation into $CD45^-CD31^-Sca1^+CD24^-$ APCs, $CD45^-CD31^-Sca1^-P\alpha^+$OPCs, and $CD45^-CD31^-Sca1^+CD24^+$ MSCs of live cells isolated from femurs of 3-month-old male $TrkA^{wt}$ and $TrkA_{Avil}^{-/-}$ mice. (E) Representative dot plot images of flow cytometry for $BrdU^+$ incorporation, (F-H) quantitative analysis of $BrdU^+$ incorporation into $CD45^-CD31^-Sca1^+CD24^-$ APCs, $CD45^-CD31^-Sca1^-P\alpha^+$OPCs, and $CD45^-CD31^-Sca1^+CD24^+$ MSCs of live cells isolated from femurs of 3-month-old male $EP4^{wt}$ and $EP4_{Avil}^{-/-}$ mice, (I) Representative dot plot images of flow cytometry for $BrdU^+$ incorporation, (J-L) quantitative analysis of $BrdU^+$ incorporation into $CD45^-CD31^-Sca1^+CD24^-$ APCs, $CD45^-CD31^-Sca1^-P\alpha^+$OPCs, and $CD45^-CD31^-Sca1^+CD24^+$ MSCs of live cells isolated from femurs of 3-month-old male $COX2^{wt}$ and $COX2_{OCN}^{-/-}$ mice mice. (M-N) Representative flow cytometry histograms and quantitative analysis for live dead cells staining by live dead kit, right part represents dead cells labeled by Alexa Fluor 350. $N \geqslant 6$ per group, $*P<0.05$ (Student t-test).

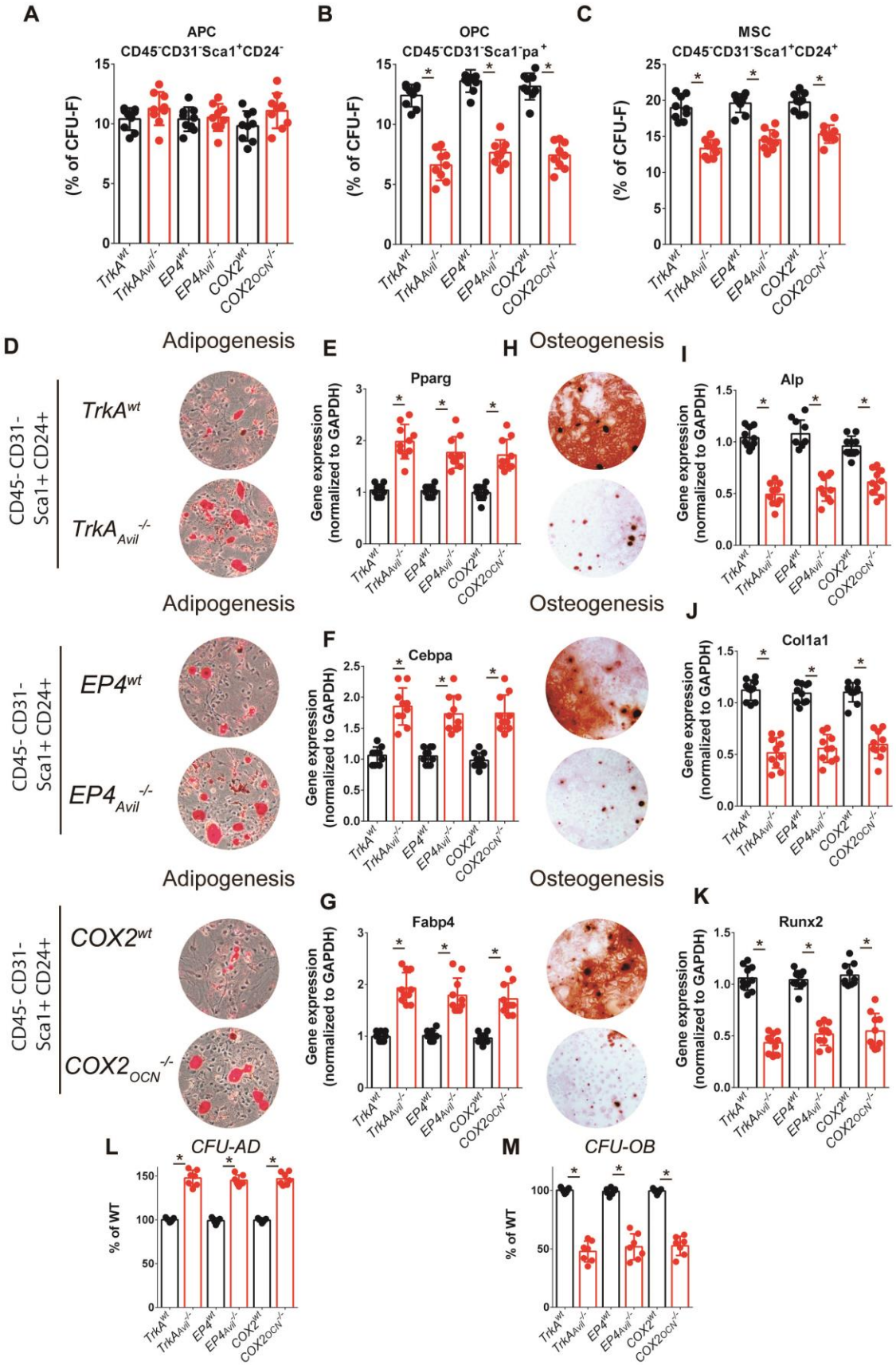
A
APC
CD45-CD31-Sca1+CD24-
(% of CFU-F)
B
OPC
CD45-CD31-Sca1-pa+
(% of CFU-F)
C
MSC
CD45-CD31-Sca1+CD24+
(% of CFU-F)
TrkAwt
TrkAAvil-/-
EP4wt
EP4Avil-/-
COX2wt
COX2OCN-/-
D
Adipogenesis
CD45- CD31- Sca1+ CD24+
TrkAwt
TrkAAvil-/-
EP4wt
EP4Avil-/-
COX2wt
COX2OCN-/-
E
Pparg
Gene expression (normalized to GAPDH)
H
Osteogenesis
I
Alp
Gene expression (normalized to GAPDH)
F
Cebpa
Gene expression (normalized to GAPDH)
J
Col1a1
Gene expression (normalized to GAPDH)
G
Fabp4
Gene expression (normalized to GAPDH)
K
Runx2
Gene expression (normalized to GAPDH)
L
CFU-AD
% of WT
M
CFU-OB
% of WT

Supplemental Figure 3:

(A-C) Quantitative analysis of percentage of CFU-F of the sorted APC, OPC and MSC from 3-month-old *TrkA*^{wt} and *TrkA*$_{Avil}^{-/-}$, *EP4*^{wt} and *EP4*$_{Avil}^{-/-}$, *COX2*^{wt} and *COX2*$_{OCN}^{-/-}$ mice. (D) Representative images and (L) quantitative analysis of oil red O for adipocytes differentiated from sorted CD45^{-}CD31^{-}Sca1^{+}CD24^{+} MSCs from 3-month-old *TrkA*^{wt} and *TrkA*$_{Avil}^{-/-}$, *EP4*^{wt} and *EP4*$_{Avil}^{-/-}$, *COX2*^{wt} and *COX2*$_{OCN}^{-/-}$ mice. (E-G) qPCR analysis of adipogenesis- and (I-K) osteogenesis-related gene expression in sorted CD45^{-}CD31^{-}Sca1^{+}CD24^{+} MSCs isolated from 3-month-old male *TrkA*^{wt} and *TrkA*$_{Avil}^{-/-}$, *EP4*^{wt} and *EP4*$_{Avil}^{-/-}$, *COX2*^{wt} and *COX2*$_{OCN}^{-/-}$ mice respectively. (H) Representative images and (M) quantitative analysis of alizarin red for osteoblasts differentiated from sorted CD45^{-}CD31^{-}Sca1^{+}CD24^{+} MSCs isolated from 3-month-old *TrkA*^{wt} and *TrkA*$_{Avil}^{-/-}$, *EP4*^{wt} and *EP4*$_{Avil}^{-/-}$, *COX2*^{wt} and *COX2*$_{OCN}^{-/-}$ mice. N⩾7 per group, **P*<0.05 (Student t-test).

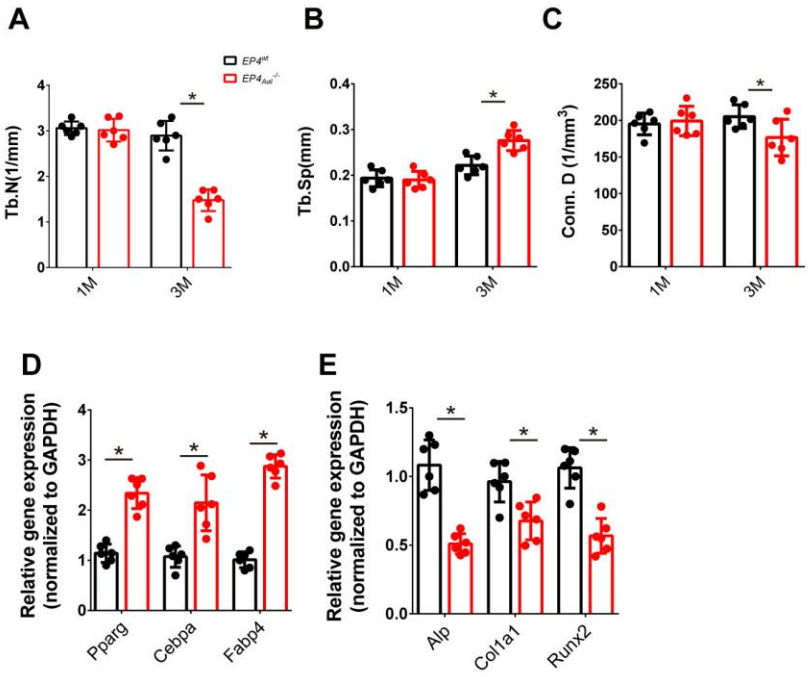

Supplemental Figure 4:

(A–C) Quantitative analysis of trabecular number (Tb. N), trabecular separation (Tb.Sp) and connectivity density (Conn. D) from 1-month-old and 3-month-old male *EP4*^{wt} and *EP4*$_{Avil}^{-/-}$ mice. (D-E) qPCR analysis of adipogenesis- and osteogenesis-related gene expression expression in MSCs isolated from 3-month-old male *EP4*^{wt} and *EP4*$_{Avil}^{-/-}$ mice. N⩾6 per group, **P*<0.05 (Student t-test).

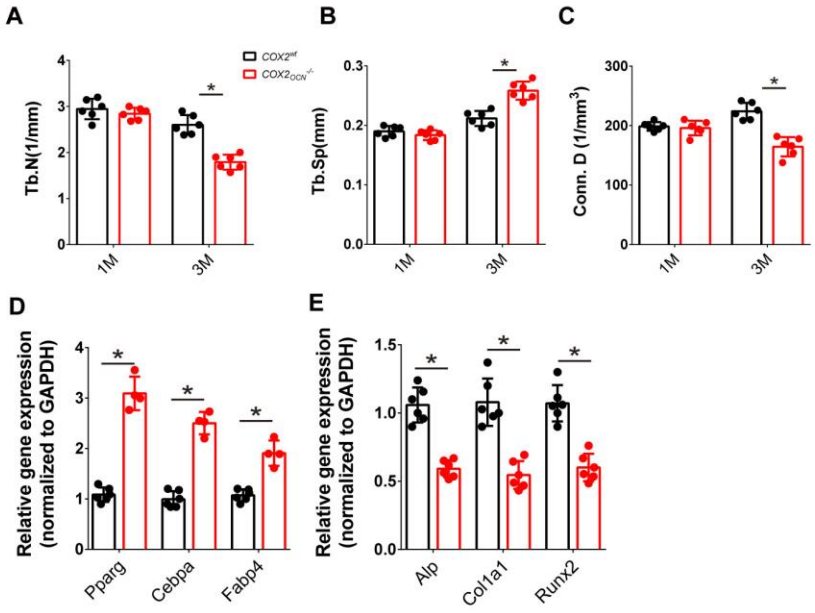

Supplemental Figure 5:

(A–C) Quantitative analysis of trabecular number (Tb. N), trabecular separation (Tb.Sp) and connectivity density (Conn. D) from 1-month-old and 3-month-old male *COX2*^{wt} and *COX2*$_{OCN}^{-/-}$ mice. (D-E) qPCR analysis of adipogenesis- and osteogenesis-related gene expression

expression in MSCs isolated from 3-month-old male *COX2*^{wt} and *COX2*$_{OCN}^{-/-}$ mice. N⩾6 per group, **P*<0.05 (Student t-test).

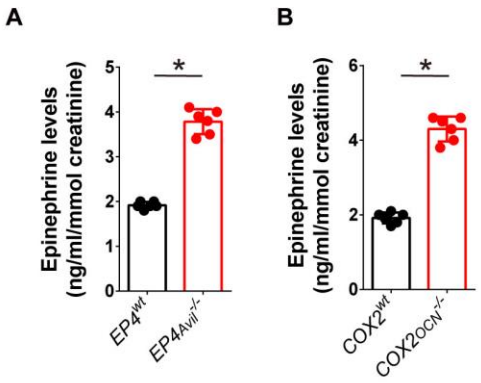

Supplemental Figure 6:

(A-B) Quantitative analysis of ELISA evaluation serum epinephrine level from 3-month-old male *EP4*^{wt} and *EP4*$_{Avil}^{-/-}$ mice and *COX2*^{wt} and *COX2*$_{OCN}^{-/-}$ mice. N⩾6 per group, **P*<0.05 (Student t-test).

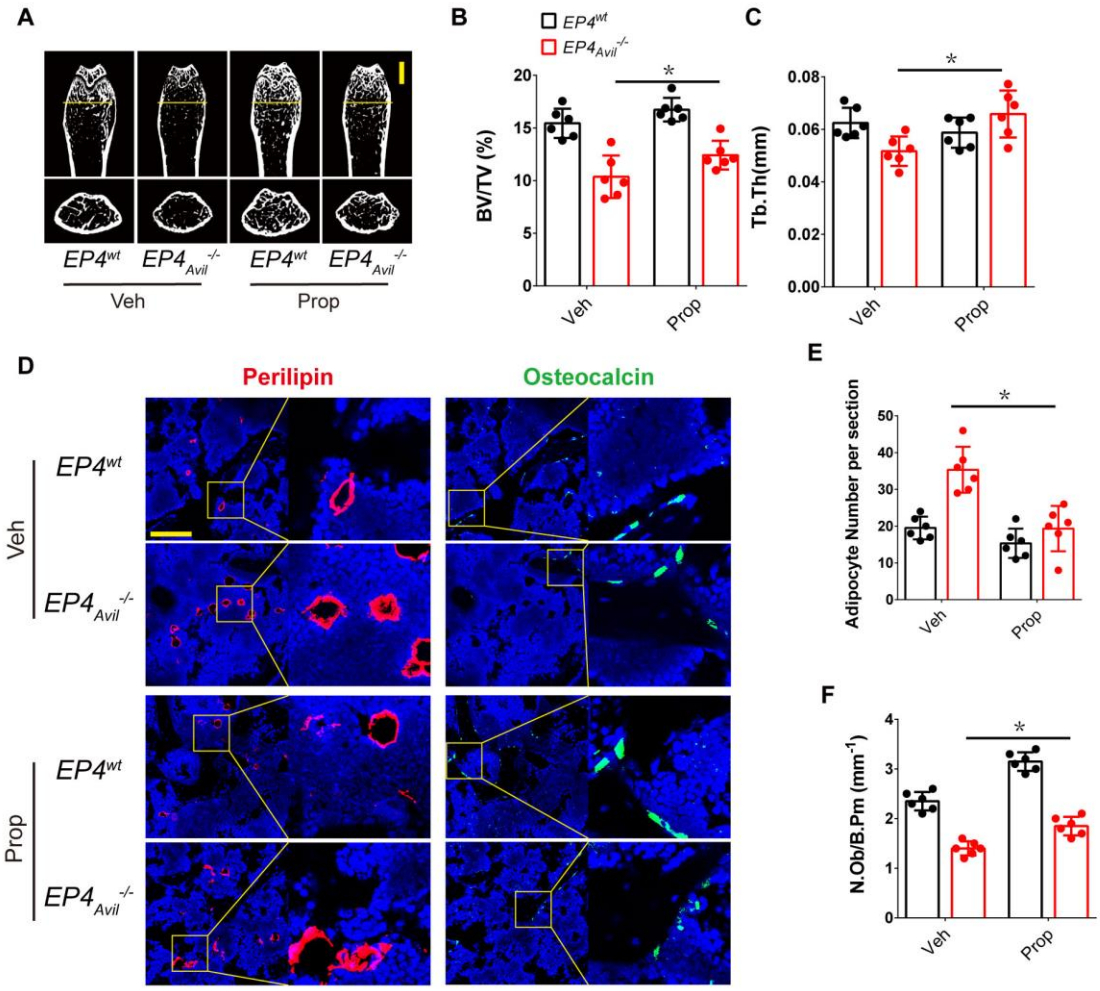

Supplemental Figure 7:

(A) Representative images and (B-C) quantitative analysis of μCT images of femurs from 3-month-old male *EP4*^{wt} and *EP4*$_{Avil}^{-/-}$ mice injected with a low dose (0.5 mg/kg per day) of propranolol or vehicle for 6 weeks, the yellow line indicated the area where the cross-section images were captured (0.5 mm proximal from the growth plate). Scale bar: 1 mm. (D) Representative images of immunohistochemical staining and (E-F) quantitative analysis of density of perilipin (red), osteocalcin (green) in femurs of 3-month-old male *EP4*^{wt} and *EP4*$_{Avil}^{-/-}$

mice injected with a low dose (0.5 mg/kg per day) of propranolol or vehicle for 6 weeks. Scale bar: 50 μm. N⩾6 per group, *P<0.05 (Two-way ANOVA for B-C, E-F).

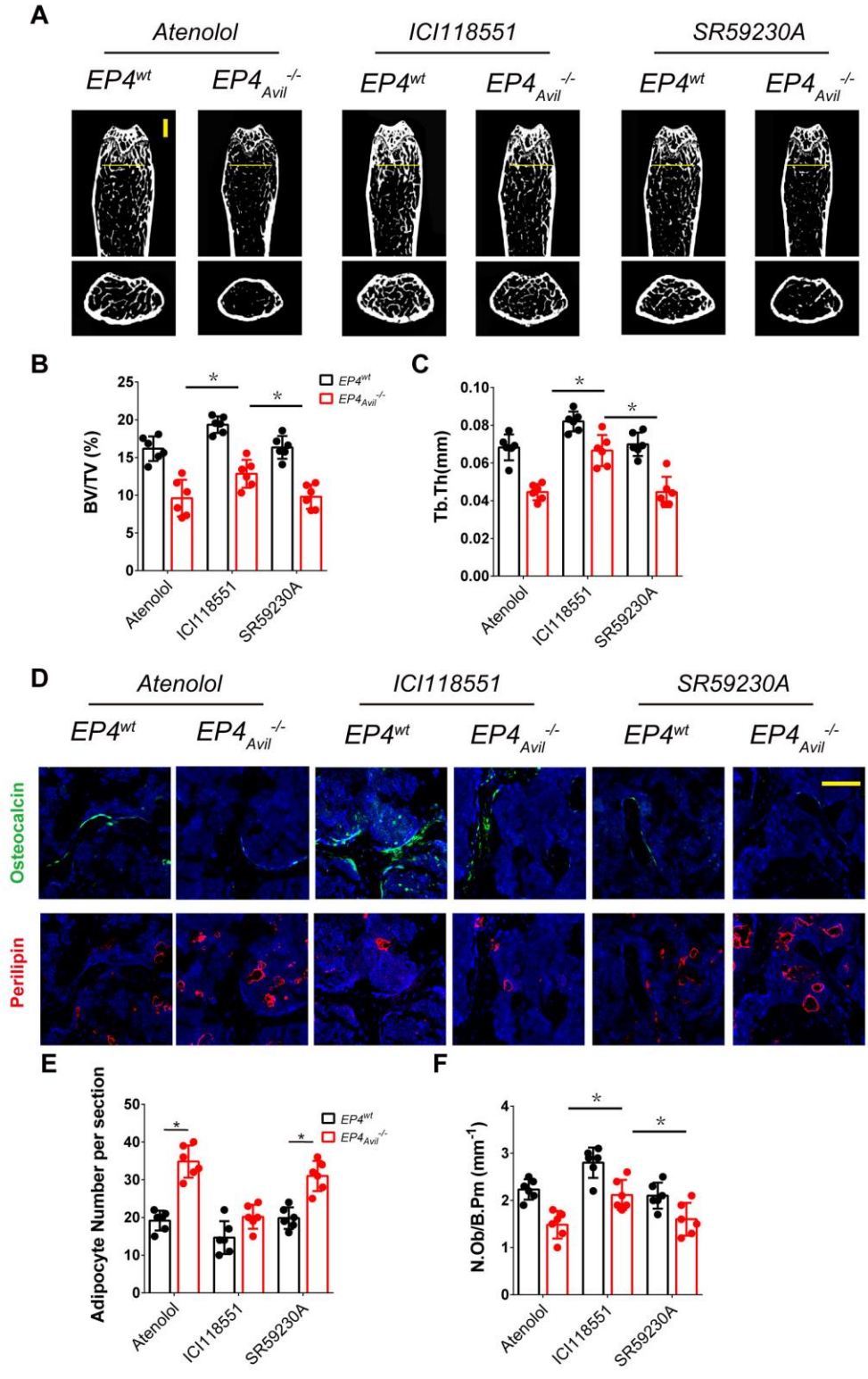

Supplemental Figure 8:

(A) Representative images and (B-C) quantitative analysis of μCT images of femurs from 3-month-old male $EP4^{wt}$ and $EP4_{Avil}^{-/-}$ mice injected with selective beta1 receptor blocker Atenolol (Tocris, 29122-68-7, given the dosage at 1mg/kg intraperitoneally), selective beta2 receptor blocker ICI118551 (Sigma, I127, given the dosage at 0.2mg/kg intraperitoneally) and selective beta3 receptor blocker SR59230A (Tocris, 1135278-41-9, given the dosage at 5mg/kg intraperitoneally) for 6 weeks, the yellow line indicated the area where the cross-section images were captured (0.5 mm proximal from the growth plate). Scale bar: 1 mm. (D) Representative images of immunohistochemical staining and (E-F) quantitative analysis of density of perilipin (red), osteocalcin (green) in femurs of 3-month-old male $EP4^{wt}$ and $EP4_{Avil}^{-/-}$ mice injected A7655 Atenolol, ICI118551 and SR59230A for 6 weeks. Scale bar: 50 μm. N⩾6 per group, *P<0.05 (Two-way ANOVA for B-C, E-F).

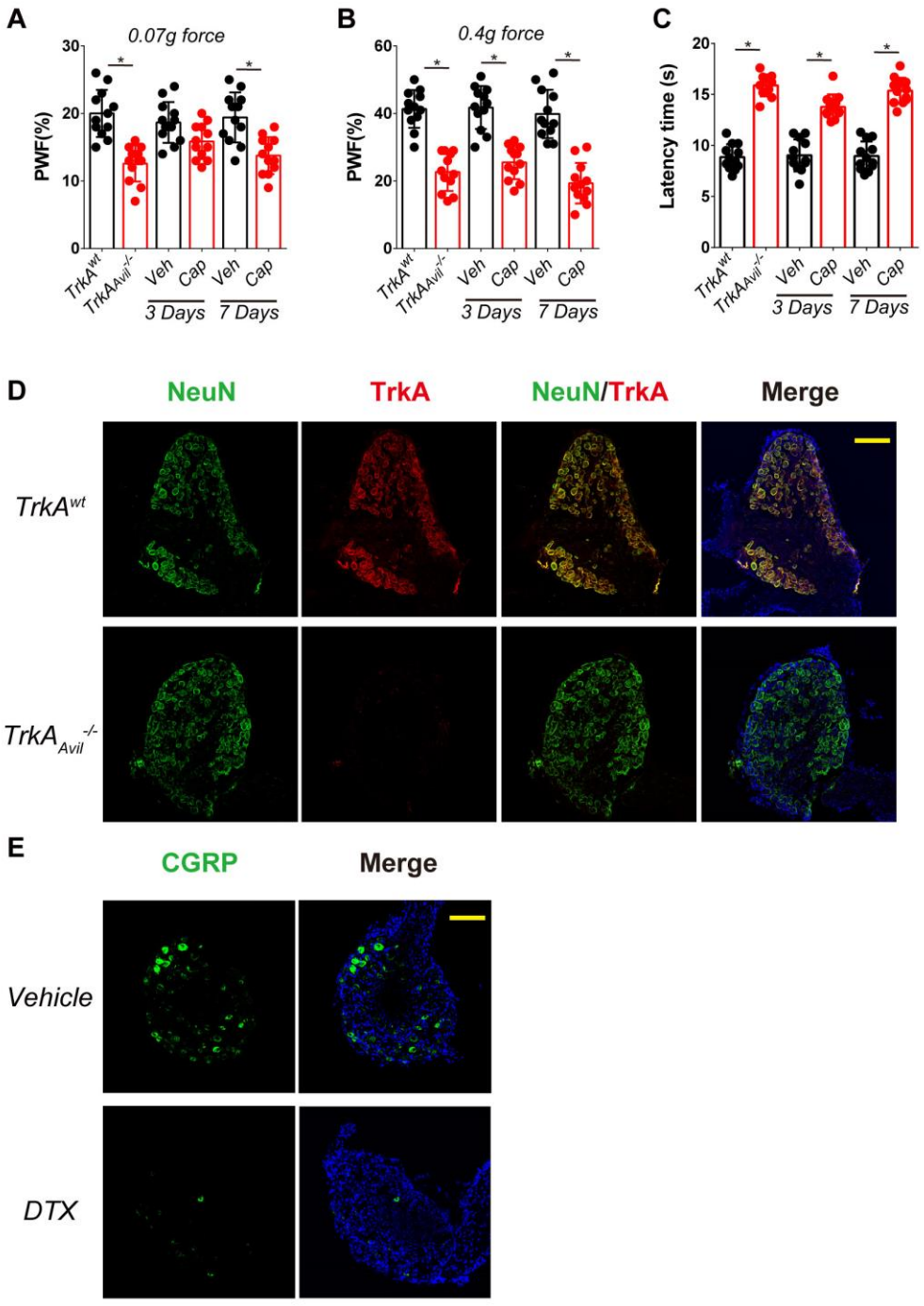

Supplemental Figure 9:

(A-B) Quantitative analysis of the frequency of paw withdrawal in response to application of 0.07 and 0.4g force via a von Frey filament of 3-month-old male *TrkA*^{wt} and *TrkA*$_{Avil}$$^{-/-}$ and 3-

month-old WT male mice injected with vehicle or capsaicin (30 mg/kg per day) for 3 and 7 days respectively. (C) Quantitative analysis of the latency time for 3-month-old male $TrkA^{wt}$ and $TrkA_{Avil}^{-/-}$ and WT male mice injected with vehicle or capsaicin (30 mg/kg per day) for 3 and 7 days in hotplate test. The latency time was defined as the time to the first sign of paw licking or jumping response. (D) Representative images of immunohistochemical staining for NeuN (Green) and TrkA (Red) and co-staining for NeuN (Green) and TrkA (Red) for the Dorsal Root Ganglion (DRG) of 3-month-old male $TrkA^{wt}$ and $TrkA_{Avil}^{-/-}$ mice. (E) Representative images of immunohistochemical staining for CGRP (Green) for DRG of of 2-month-old male $iDTR_{Avil}^{+/-}$ mice injected with 1ug per kg per day vehicle or DTX 3 time a week for four consecutive weeks. Scale bar: 100 μm. $N \geqslant 12$ per group, $*P<0.05$ (Student t-test).

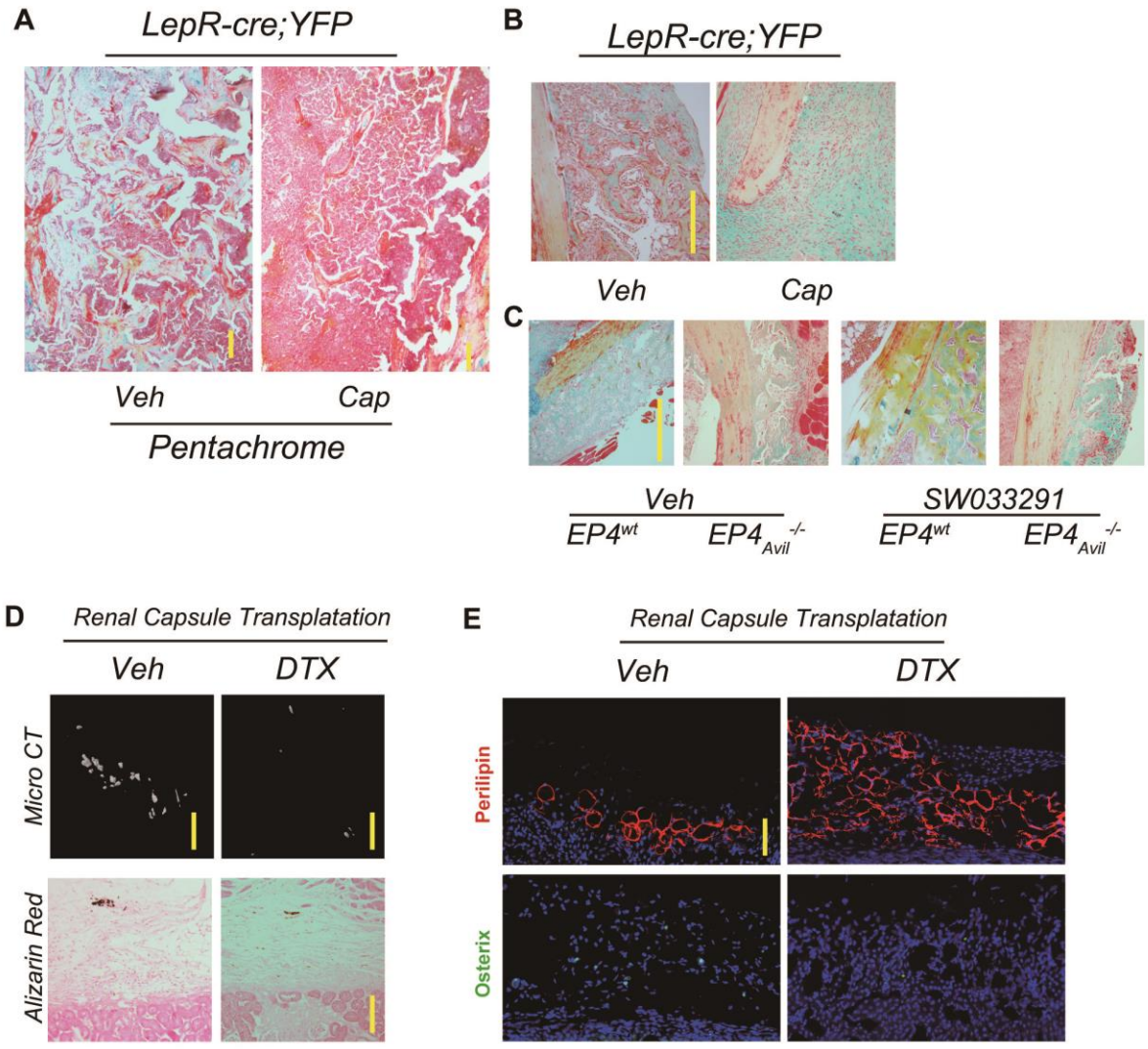

Supplemental Figure 10:

(A) Representative Movat-Pentachrome staining images in the bone regeneration area of 3-month-old male *LepR-cre;YFP* mice treated with capsaicin or vehicle 7 days after bone marrow ablation, yellow to light red area represent as trabecular bone and woven bone area, while red area represent as bone marrow. Scale bar: 100 μm. (B) Representative Movat-Pentachrome staining images in the fracture healing area of 3-month-old male *LepR-cre;YFP* mice treated with capsaicin or vehicle 7 days. (C) Representative Movat-Pentachrome staining images in the

fracture healing area of 3-month-old male $EP4^{wt}$ and $EP4_{Avil}^{-/-}$ mice treated with SW033291 or vehicle respectively after bone fracture model created for 2 weeks. Scale bar: 50 μm. (D) Representative μCT images of renal capsule of recipients of immunodeficient WT mice injected with sorted $CD45^{-}CD31^{-}Sca1^{+}CD24^{+}$ MSCs for 6 weeks which from femurs of 3-month-old $iDTR_{Avil}^{+/-}$ mice injected with 1ug per kg per day vehicle or DTX for 4 weeks. (Scale bar of μCT images: 2 mm) (E) Immunohistochemical staining of perilipin (red) osteocalcin (green) in renal capsule of recipients of immunodeficient WT mice injected with sorted $CD45^{-}CD31^{-}Sca1^{+}CD24^{+}$ MSCs for 6 weeks which from femurs of 3-month-old $iDTR_{Avil}^{+/-}$ mice injected with 1ug per kg per day vehicle or DTX for 4 weeks. Scale bar: 20 μm.

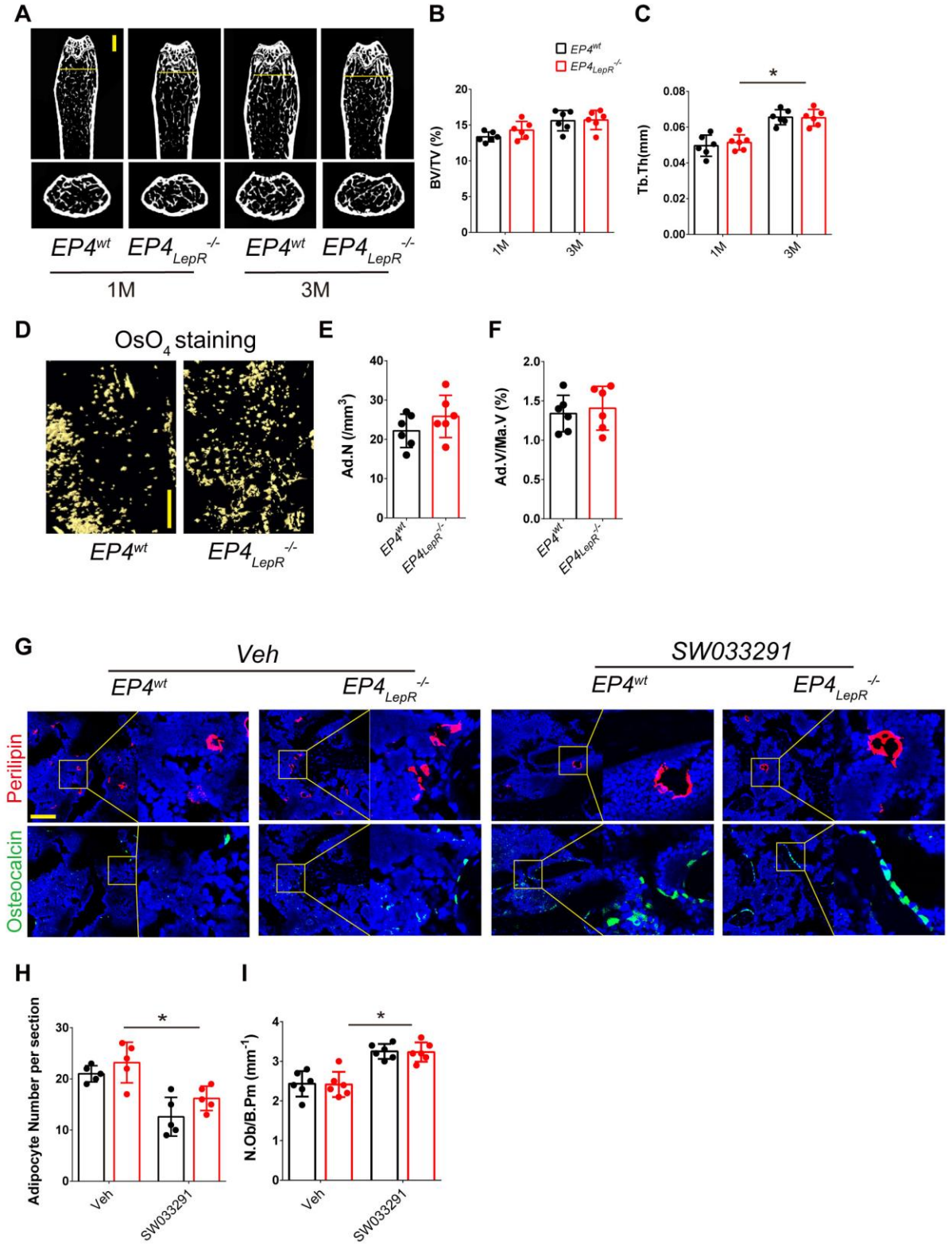

Supplemental Figure 11:

(A-C) Representative μCT images of femurs from 1-month-old and 3-month-old male $EP4^{wt}$ and $EP4_{LepR}^{-/-}$ mice. Quantitative analysis of trabecular bone fraction (Tb. BV/TV) and trabecular bone thickness (Tb.Th) , the yellow line indicated the area where the cross-section images were captured (0.5 mm proximal from the growth plate). Scale bar: 1 mm. (D–F) Representative μCT-detected OsO_4-stained images of decalcified femurs and quantitative analysis of number of adipocytes (Ad.N) and adipocyte volume/ marrow volume (Ad.V/ Ma.V) in distal femurs of 3-month-old male $EP4^{wt}$ and $EP4_{LepR}^{-/-}$ mice. Scale bar: 500 μm. (G-I) Immunohistochemical staining of perilipin (red) osteocalcin (green) in femurs of 3-month-old male $EP4^{wt}$ and $EP4_{LepR}^{-/-}$ mice treated with SW033291 and vehicle, respectively, for 1 month. Quantitative analysis of the density of perilipin and osteocalcin in femurs of 3-month-old male $EP4^{wt}$ and $EP4_{LepR}^{-/-}$ mice treated with SW033291 and vehicle, respectively. Scale bar: 50 μm. N⩾6 per group, $*P<0.05$ (Student t-test for E, F; two way ANOVA for B, C, H, I).

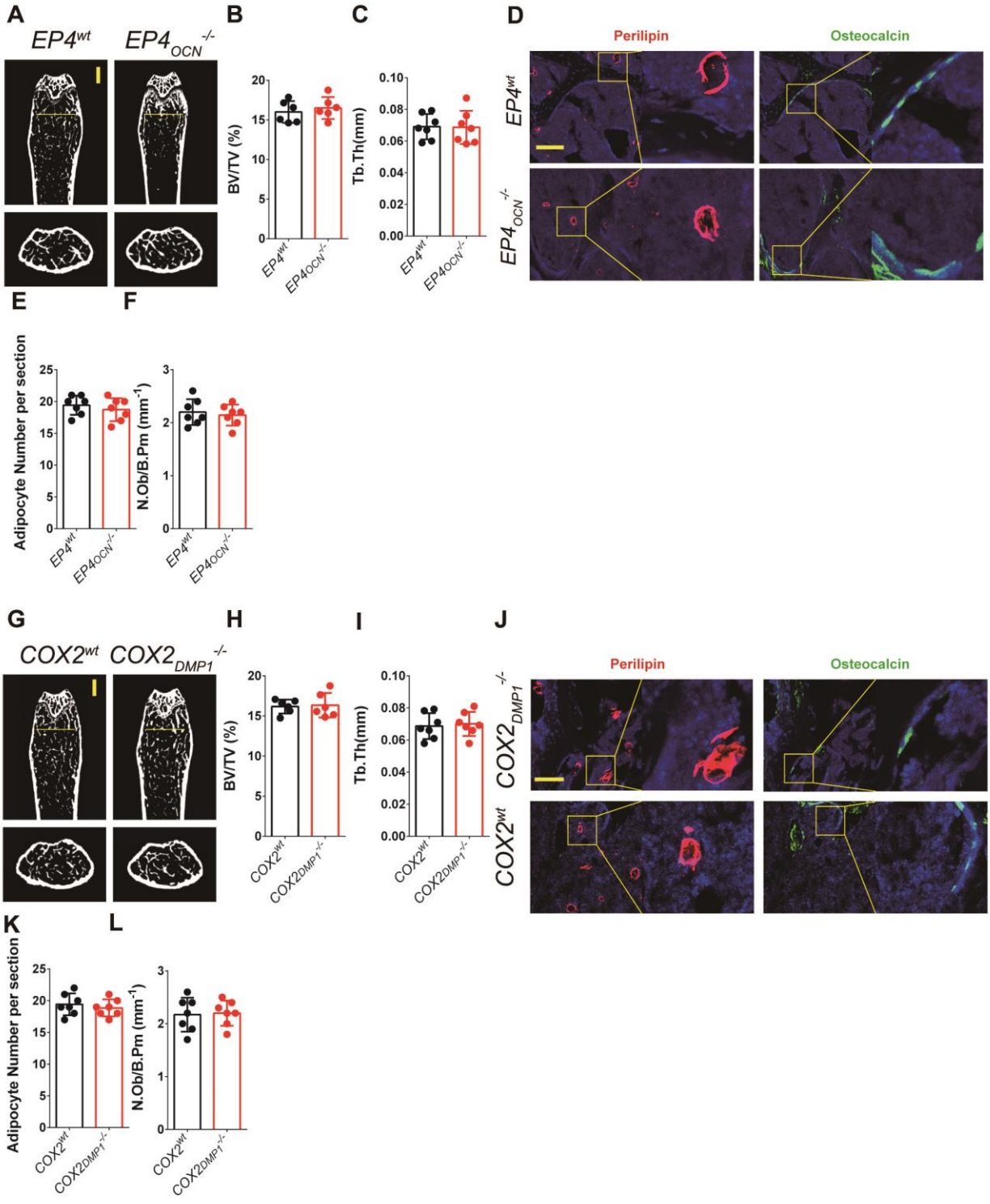

Supplemental Figure 12:

(A) Representative μCT images of femurs from 1-month-old and 3-month-old male $EP4^{wt}$ and $EP4_{OCN}^{-/-}$ mice. (B-C) Quantitative analysis of trabecular bone fraction (Tb. BV/TV) and trabecular bone thickness (Tb.Th) , the yellow line indicated the area where the cross-section images were captured (0.5 mm proximal from the growth plate). Scale bar: 1 mm. (D) Immunohistochemical staining of perilipin (red) osteocalcin (green) in femurs of 3-month-old male $EP4^{wt}$ and $EP4_{OCN}^{-/-}$ mice, (E-F) quantitative analysis of the density of perilipin and osteocalcin in femurs of 3-month-old male $EP4^{wt}$ and $EP4_{OCN}^{-/-}$ mice. Scale bar: 50 μm. (G) Representative μCT images of femurs from 1-month-old and 3-month-old male $COX2^{wt}$ and $COX2_{DMP1}^{-/-}$ mice. (H-I) Quantitative analysis of trabecular bone fraction (Tb. BV/TV) and trabecular bone thickness (Tb.Th) , the yellow line indicated the area where the cross-section images were captured (0.5 mm proximal from the growth plate). Scale bar: 1 mm. (J) Immunohistochemical staining of perilipin (red) osteocalcin (green) in femurs of 3-month-old male $COX2^{wt}$ and $COX2_{DMP1}^{-/-}$ mice, (K-L) quantitative analysis of the density of perilipin and osteocalcin in femurs of 3-month-old male $COX2^{wt}$ and $COX2_{DMP1}^{-/-}$ mice. Scale bar: 50 μm. N $\geqslant$6 per group, *P<0.05 (Student t-test).

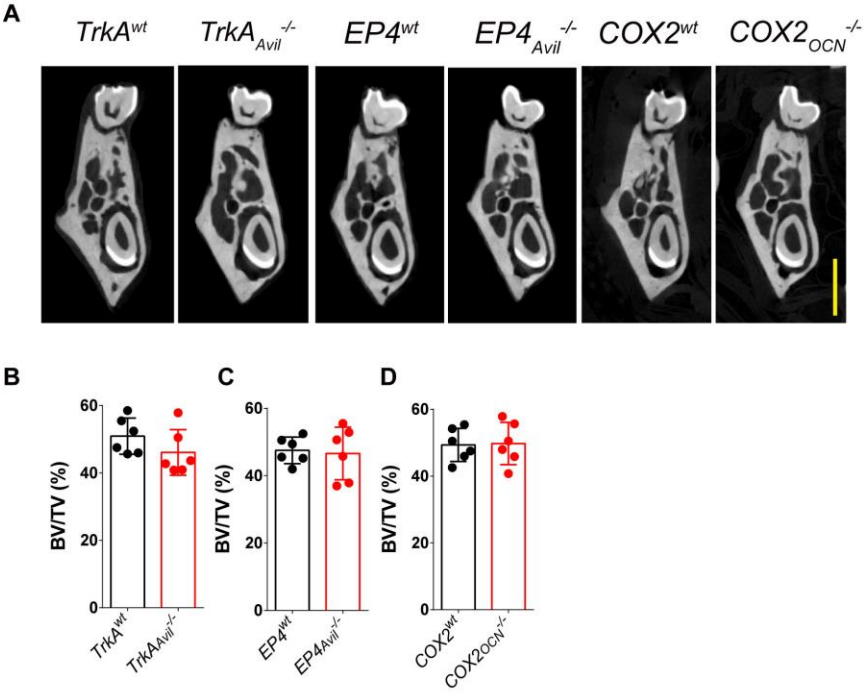
A
TrkA^wt
TrkA_Avil^-/-
EP4^wt
EP4_Avil^-/-
COX2^wt
COX2_OCN^-/-
B
C
D
BV/TV (%)
0
20
40
60
TrkA^wt
TrkA_Avil^-/-
EP4^wt
EP4_Avil^-/-
COX2^wt
COX2_OCN^-/-
E
F
BV/TV (%)
Tb.Th(mm)
0.00
0.05
0.10
10
30
0.1
1
10
100
SW033291 (mg/kg/d)
*

Supplemental Figure 13:

(A) Representative μCT images of mandibles from 3-month-old *TrkA*^{wt} and *TrkA*$_{Avil}^{-/-}$, *EP4*^{wt} and *EP4*$_{Avil}^{-/-}$, *COX2*^{wt} and *COX2*$_{OCN}^{-/-}$ mice respectively, Scale bar: 1 mm. (B-D) Quantitative analysis of trabecular bone fraction (Tb. BV/TV) of *TrkA*^{wt} and *TrkA*$_{Avil}^{-/-}$, *EP4*^{wt} and *EP4*$_{Avil}^{-/-}$, *COX2*^{wt} and *COX2*$_{OCN}^{-/-}$ mice. (E-F) Quantitative analysis of trabecular bone fraction (Tb. BV/TV) and trabecular bone thickness (Tb.Th) for the 3-month-old WT mice injected with SW033291 at a concentration of 0.1, 1, 10, 100 mg/kg/d for 1 month. N⩾6 per group, **P*<0.05. (Student t-test for B-D, two-way ANOVA for E, F)

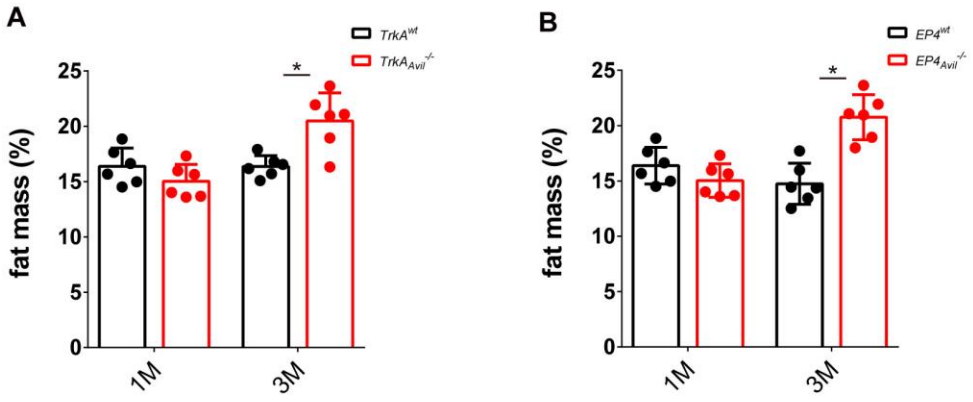

Supplemental Figure 14:

(A-B) Quantitative analysis of qNMR analysis of fat body mass of 1-month-old and 3-month-old *TrkA*^{wt} and *TrkA*$_{Avil}^{-/-}$, *EP4*^{wt} and *EP4*$_{Avil}^{-/-}$ mice. N⩾6 per group, **P*<0.05. (Student t-test)

Supplemental Method

Von Frey Test

Mechanical hyperalgesia in the glabrous skin of both hind paws was determined using von Frey filaments of 0.45g and 0.07 g (Stoelting, Wood Dale, IL). Mice were placed on a wire metal mesh grid covered with a clear plastic cage. Mice were allowed to adjust to the environment 30 min before testing. Von Frey filaments were applied to the mid-plantar surface of the hind paw through the mesh floor with enough pressure to buckle the filaments. Probing was performed only when the mouse's paw was in contact with the floor. A trial consisted of application of a von Frey filament to the hind paw 10 times at 1-sec intervals. If withdraw occurred after application, it was recorded. Mechanical withdrawal frequency was calculated as the percentage of withdrawal times in response to 10 applications.

Hot Plate Test

Thermal hyperalgesia in the glabrous hind paws skin was measured by the withdrawal latency to noxious heat stimuli simulated using a radiant source (Plantar Test Apparatus, IITC Life Science Inc., Woodland Hills, CA) with 15s cutoff latency, measured at least 3 min.

Kidney Transplantation

A 5-μl Matrigel (Corning, 356231) mixed with 10,000 sorted $CD45^{-}CD31^{-}Sca1^{+}CD24^{+}$ MSCs were placed on the ice before the operation. 2-month-old male immunodeficiency mice were anaesthetized and shaved on the left flank and sterilization at the surgical area. The kidney was externalized through a 1-cm incision and a 2-mm pocket was made in the renal capsule. The cell-Matrigel mixture was implanted underneath the capsule and the hole and incision was sealed. Animals were euthanized by CO2 after 6 weeks. Kidneys were fixed with 4% PFA for 5 h and

bone formation was detected by μCT. Samples were subjected to infiltration, embedding and section. Immunostaining was performed using standard protocol as previously described.

Metabolic Studies

Whole-body fat was measured by qNMR (Echo MRI, Phenotyping Core Lab, Johns Hopkins University School of Medicine).

ELISA Assay

The level of epinephrine in the serum was measured by Epinephrine ELISA kit. Serum was collected by centrifuge at 1500 rpm for 15 min and stored at −80℃ before analyses.